Spatial Shift and Intensification of Compound Drought and Heatwaves (CDHW) towards Southern and Eastern Tropical Regions over India

Debankana Bhattacharjee[1], Chandrika Thulaseedharan Dhanya[2*]

[1] Research Scholar, Department of Civil Engineering, Indian Institute of Technology, Delhi

[2] Professor, Department of Civil Engineering, Indian Institute of Technology, Delhi

***Corresponding author:**

Chandrika Thulaseedharan Dhanya, Professor, Department of Civil Engineering, Indian Institute of Technology Delhi, New Delhi-110016, India; Email: dhanya@civil.iitd.ac.in; Office Phone Number: +91-11-26597328.

Supplementary

S1. SNEPI (Standardized Net Precipitation and Distribution Index) (For details, refer to Singh et al., 2021)**:**

The methodology to develop the Standardized Net-Precipitation Index (SNEPI) is explained below.

- Potential evapotranspiration (PET) is subtracted from daily precipitation to ascertain the daily net precipitation. The Penman-Monteith equation is employed to acquire the PET data, which takes into account variables such as vapor pressure, ambient temperature, net radiation, wind speed, and vapor pressure deficit. The drought index's daily fluctuations are precisely represented by the daily net precipitation.
- In order to assign days as either rainy or non-rainy, a threshold is established at which the daily net precipitation balances atmospheric demand (PET) and precipitation input. During periods of excess precipitation, net precipitation values are positive, while negative values indicate deficit precipitation. The analysis encompasses all pertinent data, including single-day periods of surplus or deficit.
- The daily net-precipitation series is used to extract the magnitude, duration, and frequency of excess and deficit periods. The characteristics of deficit periods are accounted for by a weighted average of monthly net precipitation. In order to distinguish between periods with uniform precipitation and those with daily fluctuations, a uniformity coefficient is implemented to capture intra-period variability.
- For the efficient utilization of water resources, it is crucial to consider the concept of uniformity during periods of surplus or deficit. The uniformity is described by a coefficient, and the non-uniformity is quantified by the area of deviation.
- A refined monthly aggregate is produced by adjusting the initial monthly aggregate to account for the distribution of magnitudes within excess or deficit periods. The 1-month SNEPI is computed using this refined aggregate; however, the methodology can be modified to calculate SNEPI at various time scales.
- The Kolmogorov-Smirnov (KS) goodness-of-fit test is employed to evaluate four candidate distributions in order to fit the refined monthly aggregate to a suitable probability distribution function (PDF). The optimal distribution is determined by the discrepancy between the critical value and the test statistic.

Performance Analysis:

Contingency tables are generated for a variety of time periods (1, 3, 6, and 12 months) in order to evaluate the efficacy of SNEPI in comparison to SPEI. SPEI is the reference due to the absence of high-resolution official records, and its methodology is consistent with SPI. The tables delineate drought conditions according to the definitions of both indices, emphasizing the areas of agreement and disagreement. Positive disagreements arise when SNEPI suggests wetter conditions than SPEI, while negative disagreements arise when SNEPI suggests arid conditions.

The maximum level of agreement between SNEPI and SPEI is observed at the 1-month time scale, and this agreement decreases as the time scale increases. This is attributable to the growing significance of spell and frequency characteristics over extended periods. Additionally, the boxplots of SNEPI and SPEI ranges demonstrated that SNEPI significantly better depicts extreme wet and dry events across the majority of time scales. Specifically, SNEPI consistently reports heightened tails in the 1-month scale, which are associated with reduced uniformity coefficients (Uc) indicating high variability and skewed rainfall events. This emphasizes SNEPI's superior capacity to capture extreme events in comparison to SPEI, particularly at shorter time scales (Singh et al., 2021).

S2. EEMD (Empirical Ensemble Mode Decomposition)

MEEMD, which is derived from EEMD (Ensemble Empirical Mode Decomposition) and EMD (Empirical Mode Decomposition), is employed to assess the existence of any trend in each of the variables. EMD is a non-stationary, non-linear, and one-dimensional time-domain decomposition procedure. This method is highly localized and adaptive, decomposing a time series into multiple empirical modes known as intrinsic mode functions (IMFs). IMFs are oscillatory functions that are simple in nature and have a specific frequency and amplitude, which are frequently associated with a particular physical process. Additionally, IMFs must meet two criteria:

i. The number of local extrema and the number of zero crossings must be equal or at most differ by one, while the function must be symmetric in time.

ii. The mean value of the envelope, which is determined by the local maxima and local minima, must be zero.

In general, a time series is comprised of two primary components: a mono component (I) and a gradually varying component (R). The initial IMF can be derived by extracting the mono component, which is also known as IMF, through a refining process known as sifting.

Figure S1 illustrates the procedures associated with the sieving process. The process will terminate when the slow varying component is a monotonic function or when a curve contains at most one extremum, at which point no additional oscillatory component can be defined. The initial time series can be represented as:

$$Y(t) = \sum_{J=1}^{n} I_j(t) + R_n(t), \quad (1)$$

The sifting process, which is wholly dependent on the distribution of extrema, is the standard method of enforcing EMD. The results could be substantially different if the locations and values of the extrema are altered. Additionally, mode mixing may result from oscillations of disparate scales, which can result in an incorrect interpretation of the physical meaning of IMF. This unequivocally underscores the fact that EMD is susceptible to noise. The EMD approach is unstable and fails to satisfy the physical uniqueness of the decomposition methods, as we are aware that real data typically contains a certain quantity of random noise and intermittences. Ensemble Empirical Mode Decomposition (EEMD) was devised to address this limitation. This method is a noise-assisted data analysis technique. The following are the steps that are engaged in EEMD:

1. Incorporate a white noise series into the targeted data;
2. Decompose the data with the added white noise into IMFs (as outlined in EMD).
3. Repeat steps I and II on multiple occasions, each time incorporating a distinct white noise series.
4. The final result is the (ensemble) mean of the corresponding IMFs of the decompositions.

$$Trend_{EEMD}(t) = R_n(t) - R_n(1902) \quad (2)$$

S3. Results:

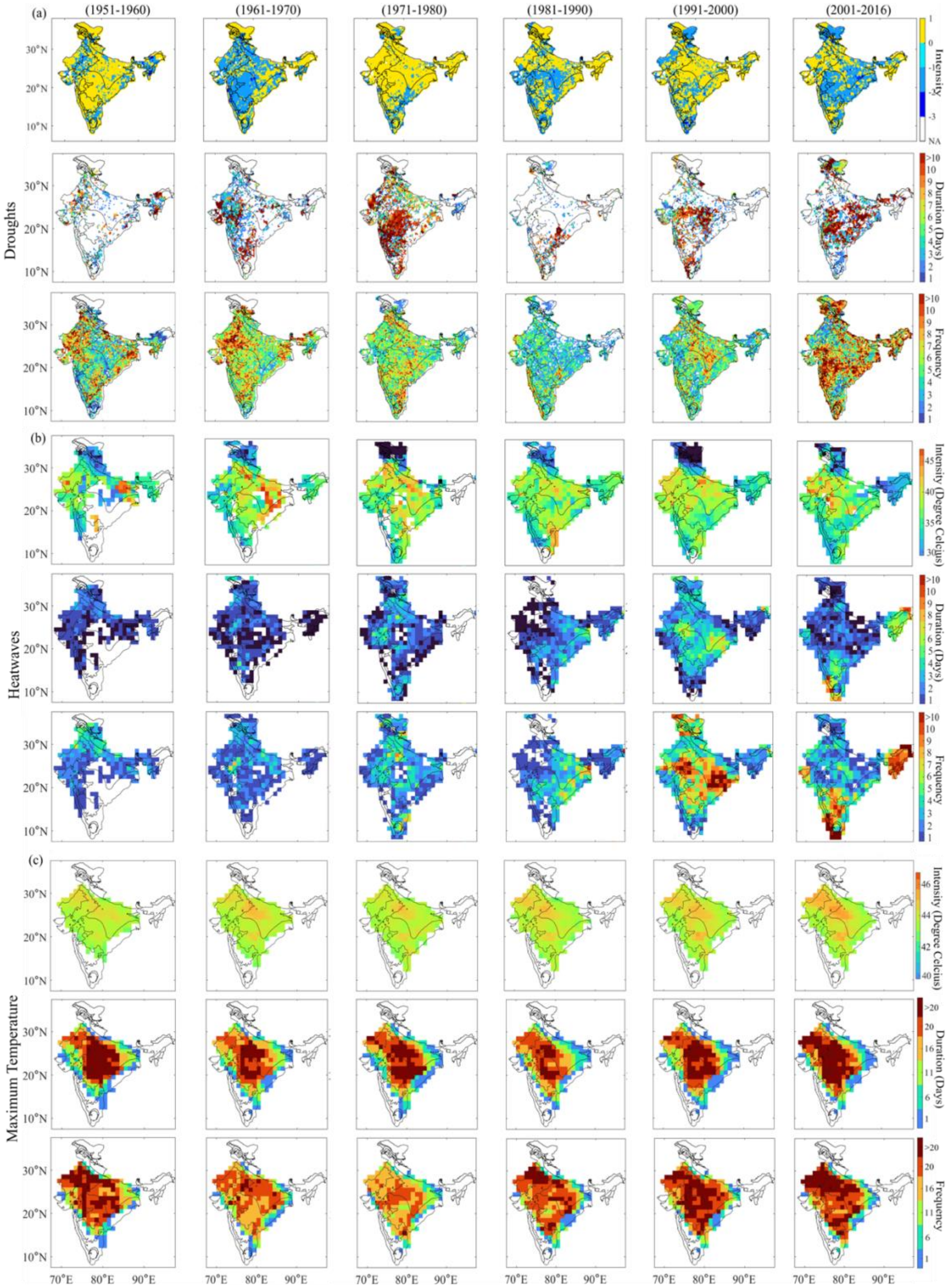

Figure S1: a) Spatiotemporal evolution of drought characteristics (intensity, duration, and frequency); b) Spatiotemporal evolution of heatwave characteristics (intensity, duration, and frequency); c) Spatiotemporal evolution of maximum temperature event characteristics (intensity, duration, and frequency) over the 6 decades starting from 1951 till 2016.

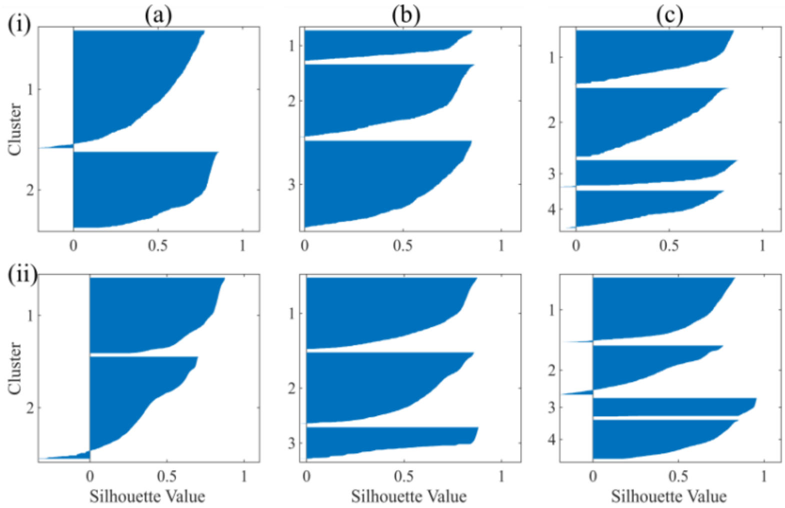

Figure S2: Silhouette plots corresponding to the heatwaves for a) 2 clusters, b) 3 clusters, c) 4 clusters, and those corresponding to the droughts for d) 2 clusters, e) 3 clusters, f) 4 clusters. The maximum number of points with high silhouette values (almost the same for all the clusters) was observed for an optimum 3 clusters for both droughts and heatwaves.

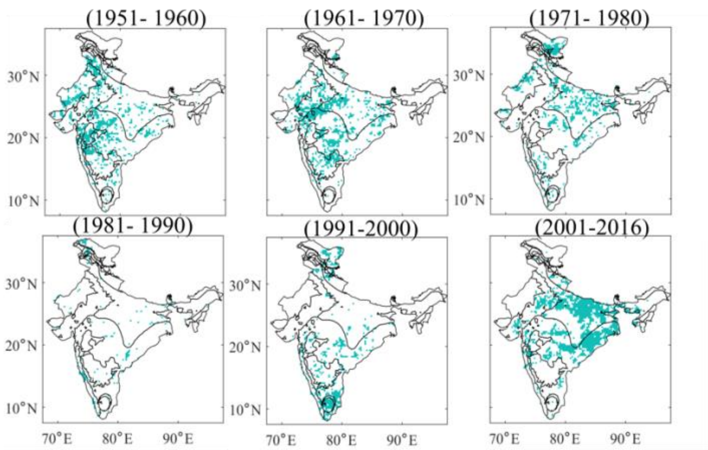

Figure S3: Spatiotemporal extent of the extracted overlapped clusters of individual droughts and heatwaves during each decade from 1951 till 2016.

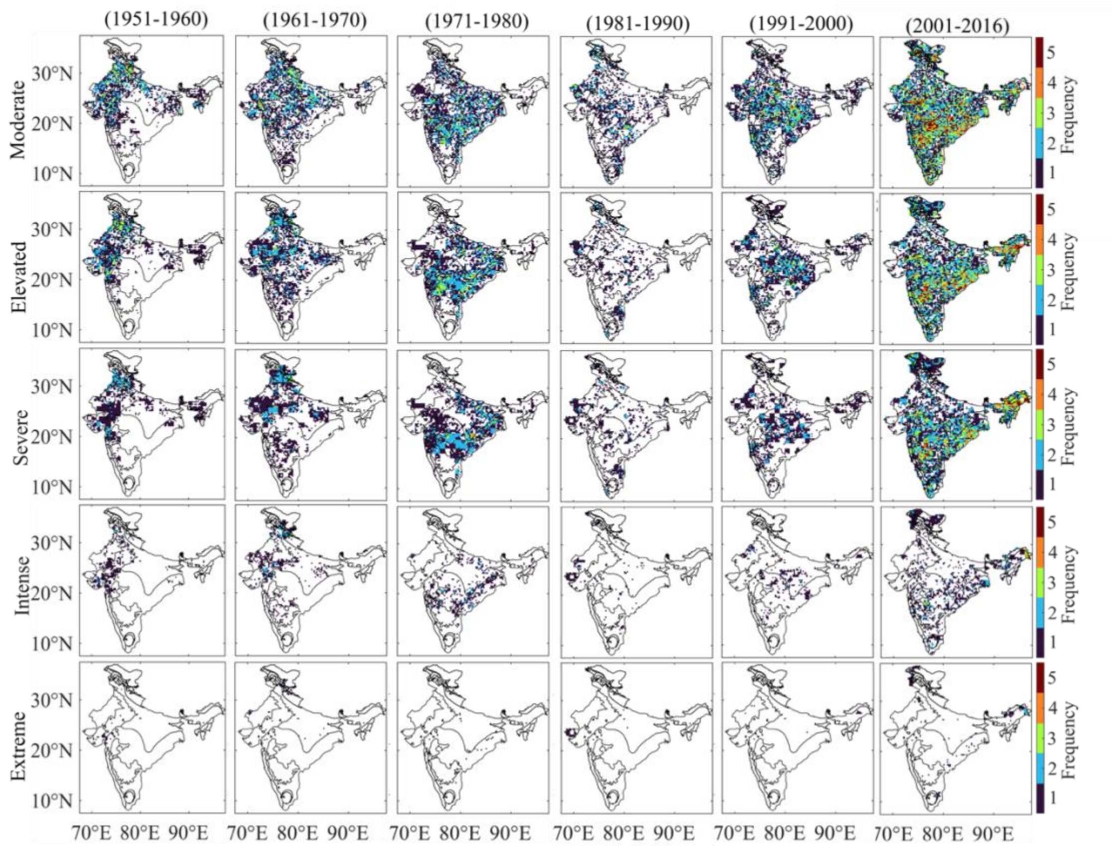

Figure S4: Spatiotemporal evolution of the different CDHW event categories (Moderate, Elevated, Severe, Intense, and Extreme) across each decade from 1951 till 2016.

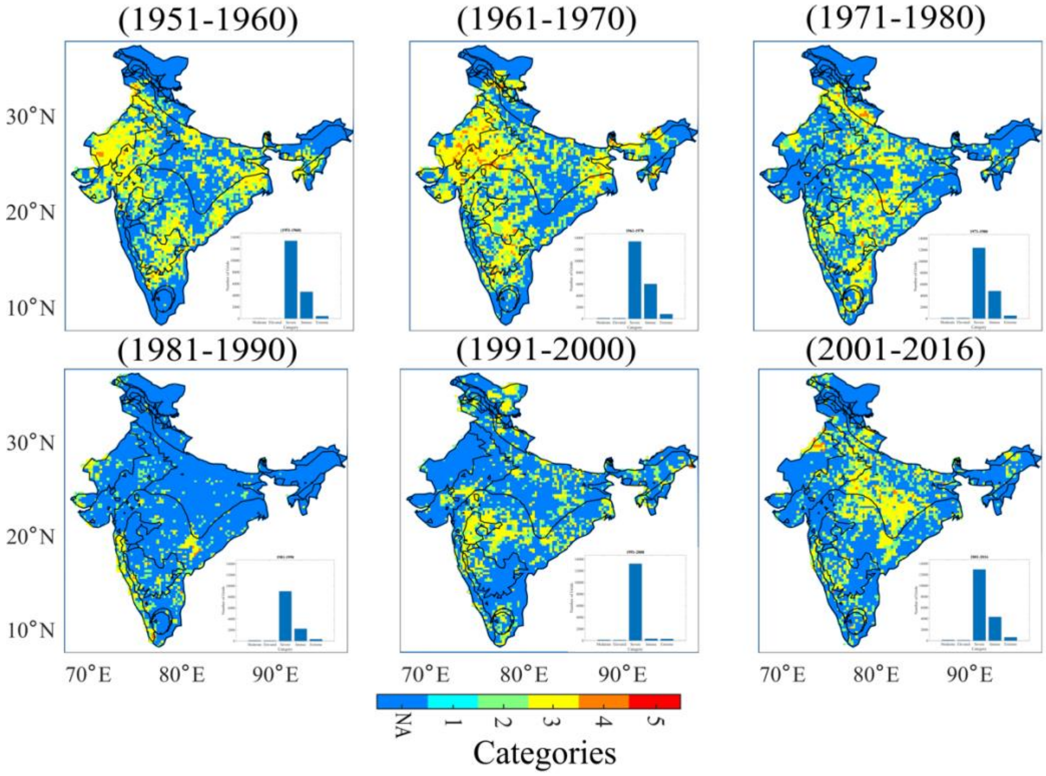

Figure S5: Spatial and decadal evolution of the dominant CDHW category across India from 1951-2016, illustrating the shifts in the most frequent event category per grid over successive decades to further highlight the intensification and spatial expansion of the different CDHW categories.

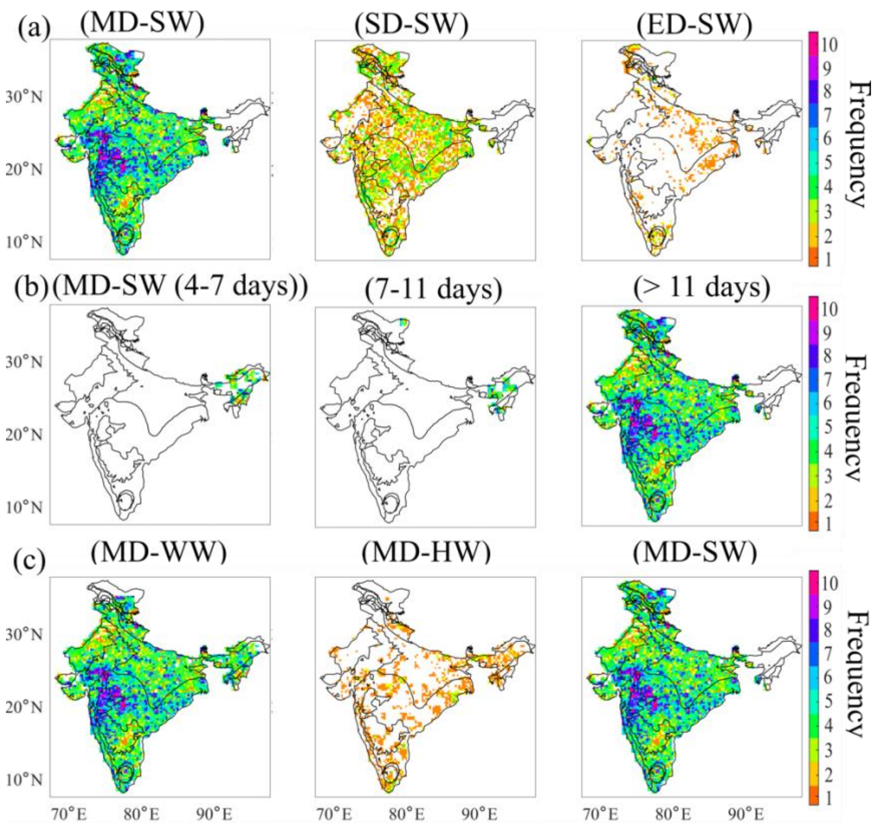

Figure S6: a) Influence of drought intensities on the compound occurrence frequency during a year for a given heatwave intensity, showing that the frequency decreased with increasing drought intensity; (b) Influence of heatwave durations on the compound occurrence frequency within a year for moderate droughts, with increase in frequency with longer duration of heatwaves except extreme east India; (c) For a given drought intensity and heatwave duration, influence of increase in temperature on the decreasing frequencies.

Possible Impacts of CDHW on population dynamics and land use/ land cover

The progression of Compound Drought and Heatwave (CDHW) occurrences in India during the last sixty years indicates changing climate patterns, regional susceptibilities, and alterations in land use and land cover (LULC). A large regional transition in CDHW occurrences from northwestern to southeastern India has profoundly impacted both physical landscapes and demographic patterns. This study assesses these changes concerning regional adaptation capacities, as described by Mohanty et al. (2021), highlighting the capacity to address increasing climate problems and formulate mitigation solutions. Urban population data from the census of India (2011) has been utilized to analyse demographic shifts in the CDHW hotspots.

Over the past 4 decades, India has experienced significant land use and land cover changes (figure 9(a)) indicating a 6% rise in urbanization and a reduction in plantation cover, especially in the dry areas of Rajasthan, where approximately the urban population which is significantly susceptible to Severe and Elevated CDHW events (figure 9(b)) has increased by almost fivefold. In West Bengal, situated in the eastern tropical wet and dry zone, urban population susceptible to Severe and Elevated CDHW conditions have increased by fourfold. Districts such as Purulia, classified as 'extreme danger' zones for heatwaves (Debnath et al., 2023), endure persistent droughts attributable to increasing temperatures and irregular precipitation patterns. Assam, notwithstanding its tropical wet and humid subtropical climate, has experienced over 10-fold urban expansion, amplifying vulnerability to intensified CDHW events due to its weak adaptation capacity. In Andhra Pradesh's semi-arid regions, the urban population at risk has risen more than fourfold, with Intense CDHW events. Kerala, notwithstanding its tropical wet environment, is experiencing heightened CDHW intensity leading to a fivefold rise in the urban population at risk. Himachal Pradesh, despite little exposure, has encountered escalating CDHW occurrences coupled with a fourfold increase in the exposed urban population (figure 9(b)).

In the realm of LULC changes, this analysis reveals a tale of transformation, with regions experiencing shifts in land cover and population dynamics. From northwestern expanses witnessing urban expansion to the coastal regions grappling with intensified CDHW occurrences, the story of India's evolving landscape is intricately linked to its climatic challenges.

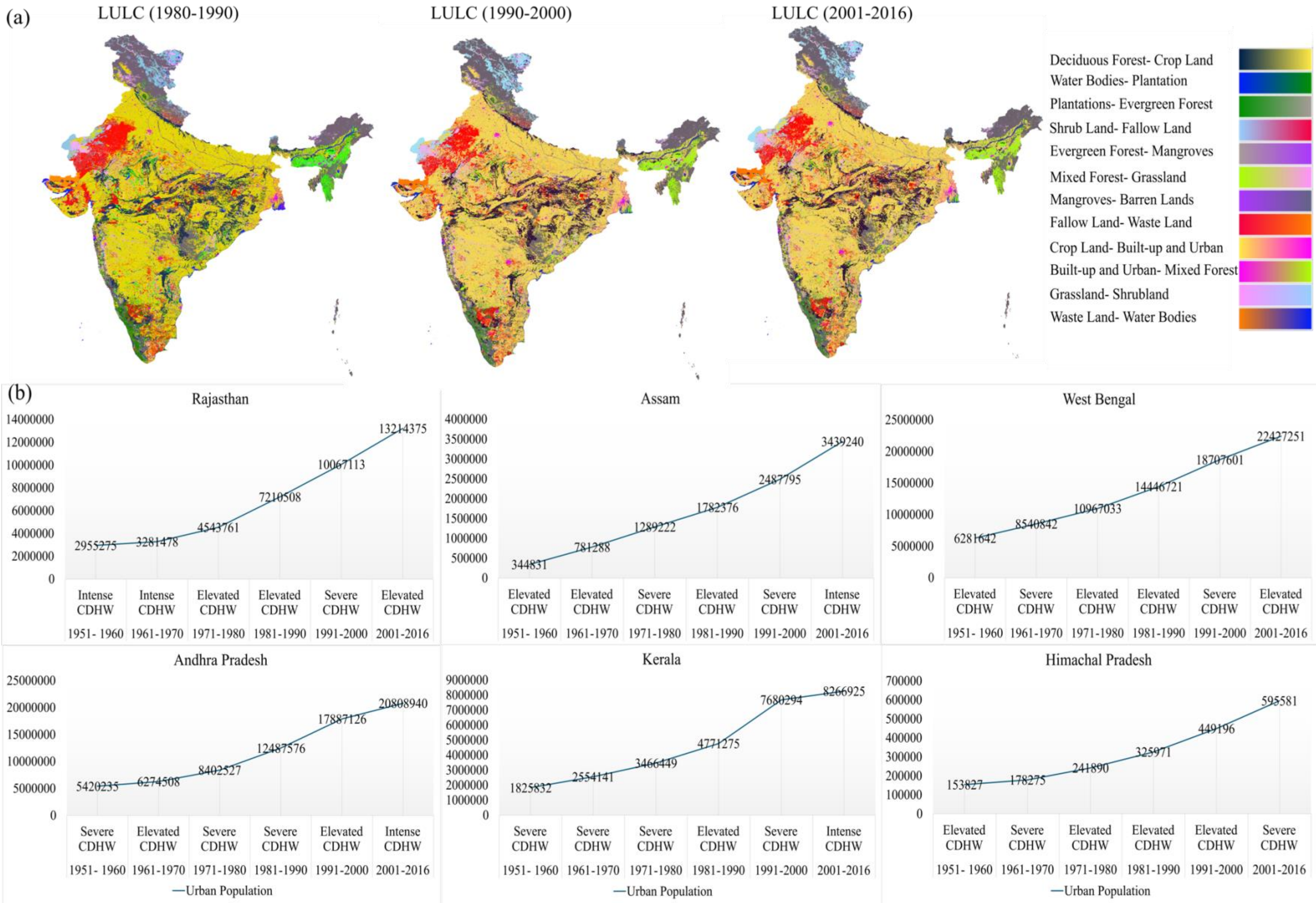
(a)
LULC (1980-1990)
LULC (1990-2000)
LULC (2001-2016)
Deciduous Forest- Crop Land
Water Bodies- Plantation
Plantations- Evergreen Forest
Shrub Land- Fallow Land
Evergreen Forest- Mangroves
Mixed Forest- Grassland
Mangroves- Barren Lands
Fallow Land- Waste Land
Crop Land- Built-up and Urban
Built-up and Urban- Mixed Forest
Grassland- Shrubland
Waste Land- Water Bodies
(b)
Rajasthan
2955275 3281478 4543761 7210508 10067113 13214375
Intense CDHW 1951- 1960
Intense CDHW 1961-1970
Elevated CDHW 1971-1980
Elevated CDHW 1981-1990
Severe CDHW 1991-2000
Elevated CDHW 2001-2016
Assam
344831 781288 1289222 1782376 2487795 3439240
Elevated CDHW 1951- 1960
Elevated CDHW 1961-1970
Severe CDHW 1971-1980
Elevated CDHW 1981-1990
Severe CDHW 1991-2000
Intense CDHW 2001-2016
West Bengal
6281642 8540842 10967033 14446721 18707601 22427251
Elevated CDHW 1951- 1960
Severe CDHW 1961-1970
Elevated CDHW 1971-1980
Elevated CDHW 1981-1990
Severe CDHW 1991-2000
Elevated CDHW 2001-2016
Andhra Pradesh
5420235 6274508 8402527 12487576 17887126 20808940
Severe CDHW 1951- 1960
Elevated CDHW 1961-1970
Severe CDHW 1971-1980
Severe CDHW 1981-1990
Elevated CDHW 1991-2000
Intense CDHW 2001-2016
Kerala
1825832 2554141 3466449 4771275 7680294 8266925
Severe CDHW 1951- 1960
Severe CDHW 1961-1970
Severe CDHW 1971-1980
Elevated CDHW 1981-1990
Severe CDHW 1991-2000
Intense CDHW 2001-2016
Himachal Pradesh
153827 178275 241890 325971 449196 595581
Elevated CDHW 1951- 1960
Severe CDHW 1961-1970
Elevated CDHW 1971-1980
Elevated CDHW 1981-1990
Elevated CDHW 1991-2000
Severe CDHW 2001-2016
Urban Population

199

Figure S7: (a) LULC dynamics across India depicts the evolving landscape of land use/land cover (LULC) across India amidst Compound Drought and Heatwave (CDHW) events during the most vulnerable decades 1981-1990, 1991-2000, and 2001-2016; (b) CDHW hotspots (states) showing increase in urban population exposure with respect to the decadal change in the CDHW intensities since 1951 till 2016.